Journal of Zhejiang University SCIENCE A
ISSN 1673-565X (Print); ISSN 1862-1775 (Online)
www.zju.edu.cn/jzus; www.springerlink.com
E-mail: jzus@zju.edu.cn

Simulation, experimental evaluation and performance improvement of a cone dielectric elastomer actuator*

Hua-ming WANG†, Jing-ying ZHU, Ke-bei YE

(*Jiangsu Key Laboratory of Precision and Micro-manufacturing Technology, Nanjing University of Aeronautics and Astronautics, Nanjing 210016, China*)

†E-mail: hmwang@nuaa.edu.cn

Received Sept. 17, 2008; Revision accepted Dec. 12, 2008; Crosschecked July 24, 2009

Abstract: Dielectric elastomer actuators (DEAs) are an emerging class of polymer actuation devices and have extensive application prospect in the field of robotics because of their light weight, high efficiency and large deformation. A cone DEA is manufactured and its working principle is analyzed. To obtain the deformation of elastomer and movement of DEA in advance, a finite element method (FEM) simulation is performed first. According to the working principle, two working equilibrium points of DEA, corresponding to the displacements of DEA with voltage off and on, are obtained and validated by experiments, thus work output in a workcycle is computed. Experiments show that the actuator can respond quickly when voltage is applied and can return to its original position rapidly when voltage is released. Simulation results agree well with experimental ones and the feasibility of DEA simulation is proved, and causes for the small difference between them in displacement output are analyzed. The performance of the actuator is improved from the aspects of both displacement and force output. A diamond four-bar linkage mechanism is used as the preload part and a displacement output of 17 mm is obtained. The force output of one actuating unit is about 1.77 N, so three actuating units are assembled in parallel and the force output is heightened to as high as 5.07 N.

Key words: Dielectric elastomer (DE), Actuator, Simulation, Performance improvement
doi:10.1631/jzus.A0820666 **Document code:** A **CLC number:** TB34; TP271

INTRODUCTION

Compared with some traditional actuators, such as piezoelectric, shape memory alloy (SMA), electroactive polymer (EAP) actuators have advantages of simple structure, lightweight, high efficiency, large deformation because of direct transformation from electrical energy into mechanical work, and will be suitable for the need of actuators in robotics, biology and medicine (de Botton and Tevet-Deree, 2006).

According to the actuating principle, EAP can be generally classified into two categories (Bar-Cohen, 2001; Kornbluh *et al*., 2004): electrochemical (involving the mobility of ions) and field-activated (involving electrostatic). Because of large actuation strain and energy density, both two kinds of EAPs have attracted more and more attention. Dielectric elastomer (DE) is a member of field-activated polymer, which has a better synthetic performance, such as environmental tolerance, larger deformation, higher energy density, efficiency and faster speed of response, than does electrochemical polymer (Michel *et al*., 2007). Current studies and applications of DEA are mainly on mini-robot (Pei *et al*., 2003), valve (Jhong *et al*., 2007), pump (Goulbourne *et al*., 2003), orthotics (Herr and Kornbluh, 2004), etc.

The deformation principle of DE is illustrated in Fig.1. DE is sandwiched between two compliant electrodes, and when voltage is applied, the opposite charges on two electrodes attract each other to form an electrostatic force (Maxwell stress) on elastomer (Pelrine *et al*., 1998):

$$p = \varepsilon_0 \varepsilon_r (V / t)^2, \quad (1)$$

* Project supported by the National Natural Science Foundation of China (No. 50605031), and the Natural Science Foundation of Jiangsu Province (No. BK2008395), China

where p is electrostatic force, ε_0 and ε_r are the permittivity of free space and the relative permittivity of the elastomer, respectively, V is the applied voltage, and t is the film thickness.

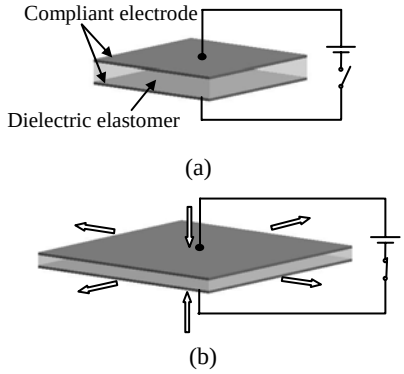

Fig.1 Deformation principle of DE. (a) Voltage off; (b) Voltage on

It is assumed that DE is incompressible and isotropic hyperelastic, so Maxwell stress makes film contract in thickness and expand in area, thus electrical energy is converted to mechanical energy. When voltage is removed, film will return to its initial dimension. Pelrine *et al*.(1998; 2000) first introduced this deformation principle into research on circular DEA. Studies on DEA began with experiments and theoretical analyses of circular DEAs, and there is still losts of literature on it now (Choi *et al*., 2005; Wissler, 2007; Wissler and Zazza, 2007). While a circular DEA has displacements in all radial directions and no structure for power output, it can only be studied for theoretical modeling and not suitable for power output.

Because of its large elongation strain of 120%~380%, high energy density of 3.4 J/g and high efficiency of 60%~90% (Kornbluh *et al*., 2004; Nam *et al*., 2007), DEAs have attracted the interests of many universities and research centers, such as Massachusetts Institute of Technology (MIT) (Vogan, 2004; Plante, 2006; Plante *et al*., 2007), Stanford Research Institute (Pei *et al*., 2003; Kofod *et al*., 2003; Kornbluh *et al*., 2004), University of Pisa (Carpi *et al*., 2006; 2007), Swiss Federal Laboratories for Materials Testing and Research (Michel *et al*., 2007; Wissler, 2007; Wisser and Zazza, 2007; Kovacs *et al*., 2007) and Sungkyunkwan University (Choi *et al*., 2005; Nam *et al*., 2007; Jung *et al*., 2007) and many kinds of actuators are presented to realize linear and rotary movements. Among current actuators, a cone DEA can provide linear displacement output and is manufactured more easily than other forms of linear actuators, such as diamond, bowtie actuators, while it has been investigated only by Artificial Muscle Inc. (Bonwit *et al*., 2006) and MIT (Plante *et al*., 2007). In Artificial Muscle Inc., two cone components, one of which is the preload for the other when actuating, are integrated into a linear actuator. In MIT, carbon fiber is used to provide the preload for actuators. To the best of our knowledge, FEM simulations are mainly on circular actuators, but not on other actuators including cone actuators. To realize the linear actuator, research on the cone actuator should be performed including experimental evaluation and FEM simulation.

MANUFACTURING AND WORKING PRINCILPLE OF CONE ACTUATORS

Manufacturing procedures of a cone actuator

As shown in Fig.2, there are three steps in the manufacturing of a cone actuator, which are simpler than those of other actuators.

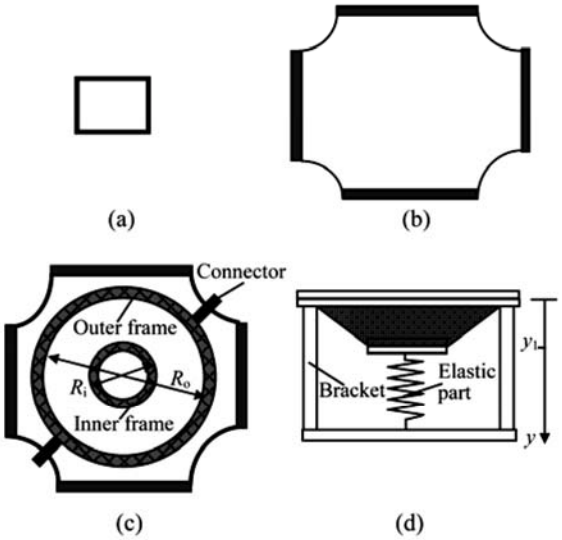

Fig.2 Manufacturing procedures of a cone DEA. (a) DE; (b) Pre-stretching; (c) Assembly; (d) Preloading
R_o: inside diameter of outer frame; R_i: outside diameter of inner frame; y_1: initial displacement

(1) Pre-stretching. DE is pre-stretched to 4×4 in two directions to obtain large deformation.

(2) Assembly. A pre-stretched elastomer is sandwiched between inner and outer frames, and two

connectors are laid between the outer frames and both sides of the elastomer, the electrode connector is made of tin-foil, which is very thin and pliable. An appropriate pressure should be applied across the bonding area to let bond strength increase.

(3) Electrode smearing and preloading. The electrode is made of carbon black EC-300J, Sylgard silicone and heptane. After the electrode is brushed by hand on both sides of the elastomer, the outer frame of the assembly is fastened to the bracket and its elastic part is connected to the inner frame as the preload, so initial displacement is produced.

VHB4910 from 3M is used, which has been proved to be of lower elastic modulus, higher dielectric constant than others, such as CF192186 from Nusil and KE441 from ShinEtsu. 2-mm thick film is manufactured by laminating two layers of 1-mm VHB4910 films. The parameters are listed in Table 1.

Table 1 Parameters of a cone DEA

Parameter	Value
Initial thickness of DE (mm)	2
Pre-stretch $\lambda_{1,\mathrm{pre}}\times\lambda_{2,\mathrm{pre}}$	4×4
Inside diameter of outer frame, R_o (mm)	90
Outside diameter of inner frame, R_i (mm)	30
Material of frame	Polycarbonate

When voltage is applied to the cone actuator shown in Fig.2d and released alternately, the inner frame of the actuator will move downwards and upwards repeatedly as shown in Fig.3.

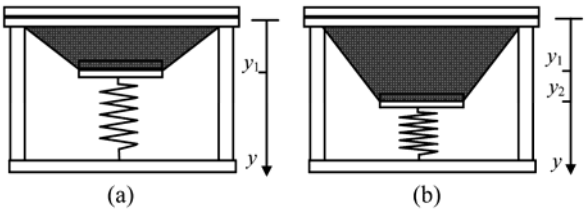

Fig.3 A cone DEA with (a) voltage off and (b) voltage on
y_1: initial displacement; y_2: displacement of actuator with voltage on

Working principle of an actuator

When voltage is applied to an actuator, the elastomer contracts in thickness and expands in area under Maxwell pressure, and when voltage is removed, the elastomer will return to its initial dimension, so the actuator can be regarded as a spring with variable stiffness (Vogan, 2004).

Fig.4 shows the working principle of a cone DEA. $f_\mathrm{t}(y)$ and $f_\mathrm{s}(y)$ are the force-displacement curves of a cone DEA with voltage off and on, respectively, and $f_\mathrm{p}(y)$ is the force-displacement curve of a preload part. The workcycle of the DEA contains two steps:

(1) Point A→C. At first, $f_\mathrm{p}(y)$ and $f_\mathrm{t}(y)$ balance each other at the equilibrium point A, which corresponds to the initial displacement d_i of the actuator under preload. When voltage is applied, stiffness of the DEA decreases quickly (point B), force difference ΔF_1 drives the inner frame to a new equilibrium point C, so displacement output d_o is produced.

(2) Point C→A. If voltage is released, stiffness of the DEA shifts upwards (point D), and force difference ΔF_2 drives the inner frame back to its initial position (point A).

Two equilibrium points A and C determine the displacement output of an actuator, hence they can be determined according to Fig.4, and validated by the actuating experiment.

Also, the area enclosed by points A, B, C and D represents the energy output obtained in a workcycle. To maximize the energy and displacement output in a work cycle, the distance between two equilibrium points A, C should be maximized.

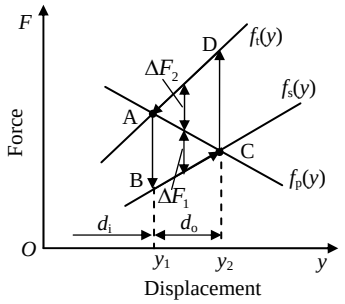

Fig.4 Working principle of DEA

FEM ANALYSIS OF CONE ACTUATORS

To analyze deformation of the elastomer and movement of the DEA, the general nonlinear FEM software ABAQUS is used for our numerical simulation.

Constitutive model

The mechanical behavior of hyperelastic materials is characterized by the strain energy function E. In this work, the Yeoh model is used, which depends on I_1, the first invariant of the left Cauchy-Green deformation tensor, descried by three material parameters C_{10}, C_{20} and C_{30}:

$$E = C_{10}(I_1 - 3) + C_{20}(I_1 - 3)^2 + C_{30}(I_1 - 3)^3, \quad (2)$$

where material parameters C_{10}, C_{20} and C_{30} are determined from uniaxial tensile tests, and are 7.0×10^{-2}, -9.0×10^{-4}, and 1.7×10^{-5} MPa, respectively (more details about the Yeoh model and its parameters in (Wissler and Mazza, 2007; Kovacs *et al*., 2007)).

Simulation results

In this simulation, elastomers are assumed to be incompressible and isotropic. Our simulation of the cone DEA includes three steps, corresponding to its manufacturing procedures:

(1) Elastomer pre-stretching. An elastomer is pre-stretched to 4×4 by imposing the displacement of the nodes on model boundary.

(2) Preloading. The deformation result of the first step is used as the input to this step. The nodes of its outer boundary are fixed in three translational degrees and the circular area at its center is hardened, then a preload of 1.96 N is applied on the area. As shown in Fig.5, an initial displacement d_i of 11.29 mm is produced.

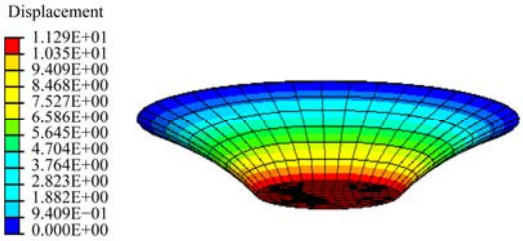

Fig.5 Initial position with preloading

(3) Voltage application. Maxwell force, computed according to Eq.(1), is exerted on the elastomer. Fig.6 shows that the displacement output is 5.47 mm.

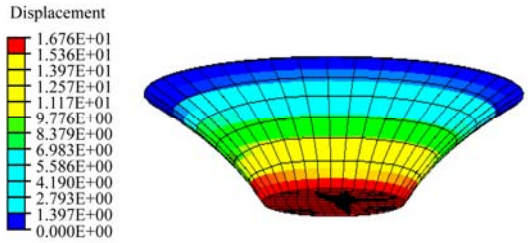

Fig.6 Total displacement with voltage application

Stress and strain distributions

Figs.7 and 8 give the von Mises stress and maximum principal strain contour plots of the elastomer, which both show that the annular area close to the inner frame has the maximum stress and strain. Fig.9 is the path plot of maximum principal strain along the radial direction Path-1 (Fig.8), which gives the position with the largest strain.

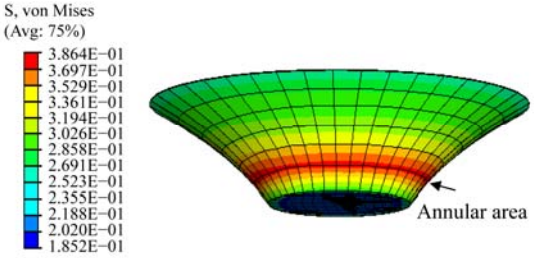

Fig.7 von Mises stress contour plot of elastomers

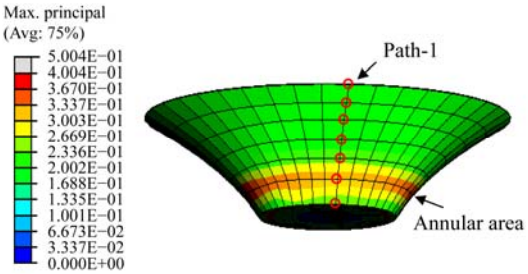

Fig.8 Max. principal strain contour plot of elastomers

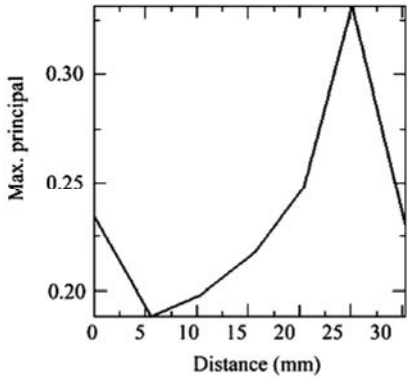

Fig.9 Max. principal strain path plot along Path-1

From Figs.7~9, a conclusion can be drawn that deformation of the elastomer is non-uniform and the largest strain of the elastomer occurs at the annular area close to its inner frame. In our experiment, a larger Maxwell force will be produced on this area than other areas because the force is inversely proportional to square of thickness of the elastomer, so the non-uniform deformation should be lessened to avoid local collapse.

EXPERIMENTAL EVALUATION OF ACTUTORS

Force-displacement curves of the actuator

The schematic diagram for measuring the force-displacement curves of the DEA is shown in Fig.10, which comprises positioning stage, force sensor, signal acquisition device and power supply. When the positioning stage moves at a given speed v, a force is acquired.

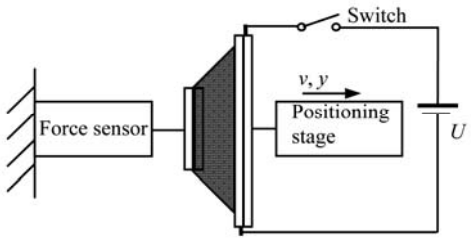

Fig.10 Schematic diagram of measurement setup

Fig.11 shows the measured force-displacement curves $f_t(y)$, $f_s(y)$, and the applied voltage for $f_s(y)$ is 9 kV. The force difference ΔF between $f_t(y)$ and $f_s(y)$ is about 1.7 N.

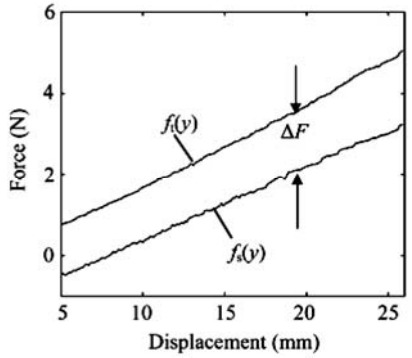

Fig.11 Force-displacement curves of a cone DEA

Equilibrium points determination

A balance weight of 200 g is used as preload in the experiment, so $f_p(y)$ is a horizontal line of 1.96 N. The preload curve has two intersection points A and C with force-displacement curves $f_t(y)$ and $f_s(y)$, respectively (Fig.12). From Section 2, points A and C are two equilibrium points corresponding to actuator displacements when voltage is off and on, respectively. The initial displacements d_i is about 12 mm and displacement output d_o is 7 mm.

Experiment of the cone actuator

The experimental setup of a cone DEA is shown in Fig.13, which contains a high-voltage power supply, balance weight of 200 g, a carbon fiber rod and a ruler. A carbon fiber rod is fastened to the inner frame as a displacement indicator, which will not influence displacement of the actuator because of light weight.

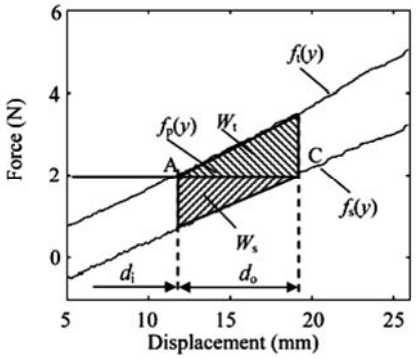

Fig.12 Equilibrium points and work output of a cone DEA
W_s: work when the actuator extends; W_t: work when the actuator retracts

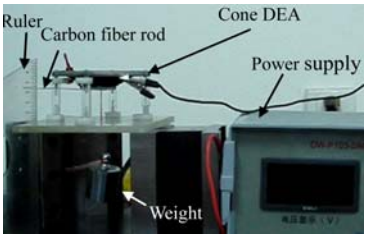

Fig.13 Experimental setup of cone DEA

When a 200-g balance weight is loaded on the inner frame, an initial displacement d_i of about 12 mm (157 mm−145 mm) is produced (Fig.14a). After 9-kV voltage is applied to the elastomer, the cone DEA responds immediately and produces a downward movement with the displacement output d_o of 7 mm (145 mm−138 mm) in about 1 s (Fig.14b). Once voltage is released, the DEA retracts to its initial position rapidly.

The experiment results for d_i and d_o coincide with the analytical results from Fig.12, so equilibrium points A and C are validated and can be used to compute work output in a workcycle.

Work output in a workcycle

The work output in a workcycle comprises two parts: work W_s when actuator extends and work W_t when the actuator retracts, as shown in Fig.12.

$$W_s = \int (f_p(y) - f_s(y))\mathrm{d}y, \tag{3}$$

$$W_t = \int (f_t(y) - f_p(y))\mathrm{d}y. \tag{4}$$

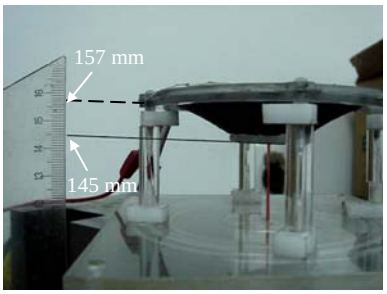

(a)

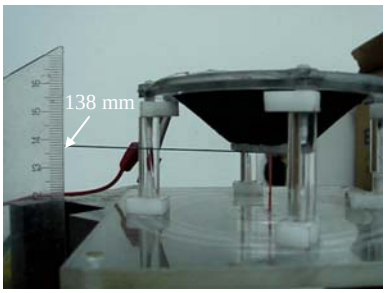

(b)

Fig.14 Experiment of a cone DEA. (a) Voltage off; (b) Voltage on

Through discrete calculation, the energy output in a work cycle is 12.3 N·mm, where W_s and W_t are 5.9 and 6.4 N·mm, respectively.

From the above calculation, the actuator with one actuating unit can only provide a small force and energy output, so a parallel assembly of multiple actuating units will enlarge the force and energy output of the DEA, but will not increase its weight obviously because the weight of an actuating unit is very small.

Discussion

From the above simulation and experiment, our simulation results agree well with the experimental results, while there is a small difference between them in displacement output, which may be caused by the following reasons:

(1) The Maxwell pressure used in the simulation is constant, while the pressure increases when the elastomer film thickness decreases, so in the future work, electro-mechanical coupling should be considered.

(2) Non-uniform deformation will make some areas, such as the annular area (Fig.8), produce larger strain than other areas because of a larger Maxwell force on them in the experiment. Some research should be made on non-uniform deformation because overlarge non-uniform deformation may cause the collapse of actuators.

In this study, a balance weight is used as the preload just for analysis convenience. The ratio of d_o to d_i is 0.58, which directly depends on the form of preload and is still very low. To make full use of the large-strain advantage of DE for d_o but not d_i, a suitable form of preload is needed to increase the ratio.

PERFORMANCE IMPROVEMENT OF DEA

The performance improvement of actuators includes two parts: displacement output improvement and force output improvement.

Displacement output improvement

Usually, an elastic part with positive stiffness (load increment has the same symbol as deformation increment), such as spring, is used as a preload for actuators. With the increase of displacement, its amount of deformation decreases, so the preload $f_p(y)$ goes downwards as Fig.4 shows and the displacement output d_o is very small. Accordingly, the preload part with negative stiffness is needed to enlarge the distance between two equilibrium points, i.e., the preload goes upwards with the increase of displacement although the amount of deformation of the elastic part decreases.

A diamond four-bar mechanism shown in Fig.15a is used to realize negative stiffness. Four rigid bars are linked by flexure joints.

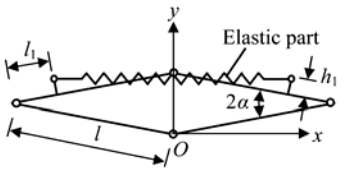

(a)

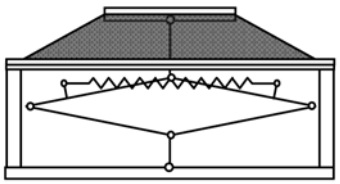

(b)

Fig.15 Schematic view of (a) diamond four-bar linkage mechanism and (b) assembly of mechanism

A coordinate system is constructed in Fig.15a and force output in y direction is obtained using the principle of virtual work:

$$f_p(y)=\frac{k(s-s_0)((l-l_1)\sin\alpha-h_1\cos\alpha)}{l\cos\alpha}, \quad (5)$$

where α=arcsin(y/(2l)), k is the elastic coefficient, s and s_0 are the current and original lengths of the elastic part, respectively.

To simplify the deduction, set l_1 and h_1 to 0.

$$f_p(y)=k(s-s_0)\tan\alpha=\frac{k(s-s_0)\sqrt{4l^2-s^2}}{s}. \quad (6)$$

The stiffness of the negative stiffness mechanism is obtained by finding a derivative of Eq.(6):

$$\frac{\mathrm{d}f_p}{\mathrm{d}s}=-\frac{k(s^3-4l^2s_0)}{s^2\sqrt{4l^2-s^2}}. \quad (7)$$

According to Eq.(7), if $s^3>4l^2s_0$, then negative stiffness is implemented. Actually, the condition $s^3>4l^2s_0$ can be satisfied easily.

Fig.16 shows our experiment of the actuator with a four-bar linkage mechanism. Initial displacement is 10 mm and displacement output is 17 mm (85 mm−68 mm), which are more than two times of that with a constant preload in Fig.14, thus the ratio of d_o to d_i is heightened to 1.7.

Force output improvement

The maximum force output of the actuator in Fig.16 is about 1.77 N. To increase the force capability of DEA, three actuating units are assembled in parallel as shown in Fig.17, while the increase of the total weight of DEA is very small, therefore, the power-mass ratio can be improved greatly. The displacement output is still about 17 mm.

Fig.18 illustrates the force output of a moving actuator. The curve $F_s(y)$ under horizontal line 0 is the force output (push force) when voltage is applied to the actuator, and the curve $F_t(y)$ above horizontal line 0 is force output (pull force) when voltage is released. The maximum force output is about 5.07 N, which is almost three times as much as that of actuator with one actuating unit.

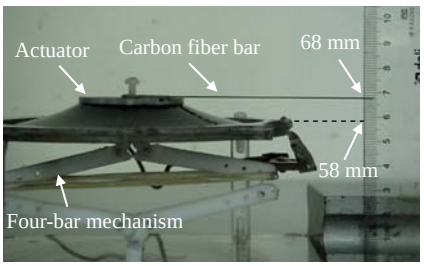

(a)

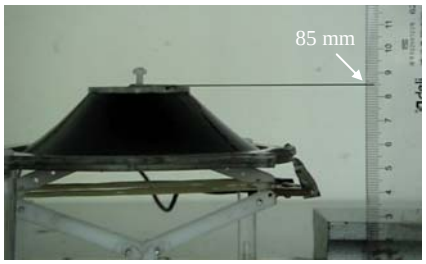

(b)

Fig.16 A cone DEA with four-bar linkage mechanism. (a) Voltage off; (b) Voltage on

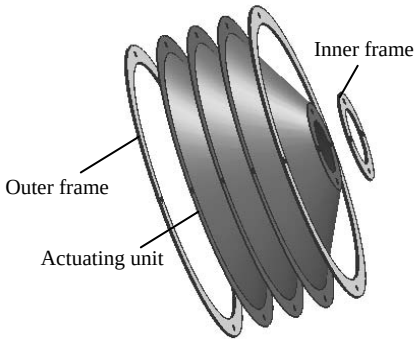

Fig.17 Structure of a cone DEA with three actuating units

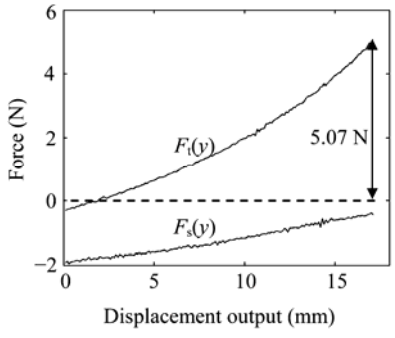

Fig.18 Force output of a actuator with three actuating units

CONCLUSION

A cone DEA is designed and manufactured. To obtain the displacements of the actuator in advance, an FEM simulation is performed to predict the movement of the actuator. Based on the working principle of the actuator, its displacement output and initial displacement are determined through the analysis on the relationship between force-displacement curves and preload of the actuator, which are about 7 and 12 mm, respectively, and are in accord with experimental results; and the work output in a workcycle is calculated. Also, the simulation result in initial displacement agrees well with the experimental, while there is a small difference in output displacement between them.

To make full use of the large-strain advantage of DE, the four-bar linkage mechanism is used to provide a preload. d_o of 17 mm and a ratio of 1.7 are achieved. Three actuating units are connected in parallel to increase the force output, and the maximum is 5.07 N. After further improvements of its displacement and force output, the cone actuator will be used as an actuating device in hopping robots, in which the preload part will be replaced by four lightweight carbon fiber bars.

Even though DEA works under a quite low current, high voltages needed for the actuator might be a barrier for the application of DEA because some problems will occur in design and security, then it is imperative to research the preparation of low-voltage actuating elastomers.

References

Bar-Cohen, Y., 2001. Electroactive Polymer (EAP) Actuators as Artificial Muscles-Reality, Potential and Challenges. SPIE Press, WA, USA.

Bonwit, N., Heim, J., Rosenthal, M., Duncheon, C., Beavers, A., 2006. Design of Commercial Applications of EPAM Technology. Proceedings of SPIE Electroactive Polymer Actuators and Devices, San Diego, USA. SPIE, Bellingham, USA, p.616805-1-616805-10. [doi:10.1117/12.658775]

Carpi, F., Fantoni, G., Guerrini, P., de Rossi, D., 2006. Buckling dielectric ealstomer actuators and their use as motors for the eyeballs of an android face. Proceedings of SPIE Electroactive Polymer Actuators and Devices, San Diego, USA. SPIE, Bellingham, USA, p.61681A-1-61681A-6. [doi:10.1117/12.655254]

Carpi, F., Salaris, C., De Rossi, D., 2007. Folded dielectric elastomer actuators. *Smart Materials and Structures*, **16**:300-305. [doi:10.1088/0964-1726/16/2/S15]

Choi, H.R., Jung, K., Chu, N.H., Jung, M.Y., Koo, I., Koo, J., Lee, J., Lee, J., Nam, J., Cho, M., Lee, Y.K., 2005. Effects of Prestrain on Behavior of Dielectric Elastomer Actuator. Proceedings of SPIE Smart Electroactive Polymer Actuators and Devices, San Diego, USA. SPIE, Bellingham, USA, p.283-291. [doi:10.1117/12.599363]

de Botton, G., Tevet-Deree, L., 2006. Electroactive Polymer Composites-analysis and Simulation. Proceedings of SPIE Active Materials: Behavior and Mechanics, San Diego, USA. SPIE, Bellingham, USA, p.548-557. [doi:10.1117/12. 659981]

Goulbourne, N., Frecker, M., Mockensturm, E., Snyder, A., 2003. Modeling of a Dielectric Elastomer Diaphragm for a Prosthetic Blood Pump. Proceedings of SPIE Electroactive Polymer Actuators and Devices, San Diego, USA. SPIE, Bellingham, USA, p.319-331.

Herr, H., Kornbluh, R., 2004. New Horizons for Orthotic and Prosthetic Technology: Artificial Muscle for Ambulation. Proceedings of SPIE Electroactive Polymer Actuators and Devices, San Diego, USA. SPIE, Bellingham, USA, p.1-9. [doi:10.1117/12.544510]

Jhong, Y.Y., Huang, C.M., Hsieh, C.C., Fu, C.C., 2007. Improvement of Viscoelastic Effects of Dielectric Elastomer Actuator and Its Application for Valve Devices. Proceedings of SPIE Electroactive Polymer Actuators and Devices, San Diego, USA. SPIE, Bellingham, USA, p.65241Y-1-65241Y-9. [doi:10.1117/12.715998]

Jung, K., Koo, J.C., Nam, J., Lee, Y.K., Choi, H.R., 2007. Artificial annelid robot driven by soft actuators. *Bioinspiration & Biomimetics*, **2**(2):S42-S49. [doi:10.1088/1748-3182/2/2/S05]

Kofod, G., Kornbluh, R.D., Pelrine, R.E., Sommer-Larsen, P., 2003. Actuation response of polyacrylate dielectric elastomers. *Journal of Intelligent Material Systems and Structures*, **14**(12):787-793. [doi:10.1177/1045389X03039260]

Kornbluh, R., Pelrine, R., Prahlad, H., 2004. Electroactive Polymers: An Emerging Technology for MEMS. Proceedings of SPIE MEMS/MOEMS Components and Their Applications, San Jose, USA. SPIE, Bellingham, USA, p.13-27. [doi:10.1117/12.538382]

Kovacs, G., Lochmatter, P., Wissler, M., 2007. An arm wrestling robot driven by dielectric elastomer actuators. *Smart Materials and Structures*, **16**:S306-S317. [doi:10.1088/0964-1726/16/2/S16]

Michel, S., Dürager, C., Zobel, M., Fink, E., 2007. Electro Active Polymers as a Novel Actuator Technology for Lighter than Air Vehicles. Proceedings of SPIE Electroactive Polymer Actuators and Devices, San Diego, USA. SPIE, Bellingham, USA, p.65241Q1-11. [doi:10.1117/12.716658]

Nam, J.D., Choi, H.R., Koo, J.C., 2007. Dielectric Elastomers for Artificial Muscles. Kwang, J.K., Satoshi, T. (Eds.), Electroactive Polymers for Robotic Applications. Springer, London, p.37-48.

Pei, Q.B., Pelrine, R., Stanford, S., 2003. Electroelastomer rolls and their application for biomimetic walking robots.

Synthetic Metals, **135-136**:129-131. [doi:10.1016/S0379-6779(02)00535-0]

Pelrine, R.E., Kornbluh, R.D., Joseph, J.P., 1998. Electrostriction of polymer dielectrics with compliant electrodes as a means of actuation. *Sensors and Actuators A: Physical*, **64**(1):77-85.

Pelrine, R.E., Kornbluh, R.D., Pei, Q.B., Joseph, J., 2000. High-speed electrically actuated elastomers with over 100% strain. *Science*, **287**(5454):836-839. [doi:10.1126/science.287.5454.836]

Plante, J., Devita, L.M., Dubowsky, S., 2007. A Road to Practical Dielectric Elastomer Actuators Based Robotics and Mechatronics: Discrete Actuation. Proceedings of SPIE Electroactive Polymer Actuators and Devices, San Diego, USA. SPIE, Bellingham, USA, p.652406-1-652406-15. [doi:10.1117/12.715236]

Plante, J.S., 2006. Dielectric Elastomer Actuators for Binary Robotics and Mechatronics. PhD Thesis, Massachusetts Institute of Technology, Boston, USA.

Vogan, J., 2004. Development of Dielectric Elastomer Actuators for MRI Devices. MS Thesis, Massachusetts Institute of Technology, Boston, USA.

Wissler, M., 2007. Modeling Dielectric Elastomer Actuators. PhD Thesis, Swiss Federal Institute of Technology, Zurich, Switzerland.

Wissler, M., Mazza, E., 2007. Mechanical behavior of an acrylic elastomer used in dielectric elastomer actuators. *Sensors and Actuators A: Physical*, **134**(2):494-504. [doi:10.1016/j.sna.2006.05.024]